International Journal of Marine Engineering Innovation and Research, Vol. 11(2), June. 2026. 755-765
(pISSN: 2541-5972, eISSN: 2548-1479)

Design and Implementation Independent Battery and Lost-Link Fail-Safe Module for USV Safety

Setyawan Ajie Sukarno[1*], Hisyam Nuruliman[2], Ridwan [3]
(Received: 14 May 2026 / Revised: 18 May 2026 /Accepted: 25 May 2026 / Available Online: 29 June 2026)

***Abstract*—** Autonomous Unmanned Surface Vehicles (USVs) require reliable fail-safe mechanisms to ensure operational safety, particularly in the event of low battery conditions and communication failures. However, most existing fail-safe systems still rely on the main controller, which can render them ineffective when the main system experiences a malfunction or loss of communication. This research proposes an independent fail-safe module based on battery monitoring and lost-link detection to enhance the reliability and safety of USVs. The proposed system integrates the Jetson Orin Nano, a CUAV autopilot, and an independent ESP32-based monitoring module capable of monitoring battery conditions and communication status via MAVLink heartbeat signals. A mission-progress-based energy estimation method is applied to evaluate mission feasibility based on remaining battery capacity and travel progress. Testing was conducted under normal operating conditions, low battery conditions, and communication loss. The research results show that the voltage monitoring system achieved 99.87% accuracy, while the fail-safe mechanism successfully detected low battery conditions within 2.5–3.0 seconds and communication loss within 6–15 seconds. The system is also capable of automatically executing Return-to-Home (RTH) and Loiter modes, thereby enhancing the reliability, fault tolerance, and operational safety of autonomous USVs.

Keywords—Energy-Based Monitoring, Fail-safe Mechanism, Lost-Link Detection, Mission Feasibility, USV

**Corresponding Author: ajie@ae.polman-bandung.ac.id*

I. INTRODUCTION

The operational reliability of Unmanned Surface Vehicles (USVs) is a crucial aspect of autonomous maritime missions, particularly in long-duration and mission-critical operations [1], [2], [3]. USVs are widely used in various applications such as environmental monitoring, hydrographic surveys, and maritime surveillance, where system failures can pose significant operational risks [4], [5], [6].

Maintaining stable communication between onboard systems and the control unit is one of the main challenges in USV operations. Modern USVs rely heavily on continuous real-time data exchange for navigation and control, making them vulnerable to latency, packet loss, and communication disruptions in dynamic maritime environments. Such communication failures may result in loss of control or mission failure [7], [11], [17].

In addition to communication challenges, power management plays a critical role in ensuring reliable USV operations. Battery limitations and energy consumption significantly impact system endurance and mission performance, particularly during long-term deployments [10], [11]. Although monitoring systems have been developed to observe system parameters in real time, these systems are generally integrated into the main controller and rely on its proper functionality [11], [12].

From a systems engineering perspective, reliability and safety are closely related to the concepts of dependability and fault tolerance, whereby a system must continue to operate correctly even in the presence of faults or unexpected conditions [13], [14], [15]. However, existing approaches to system safety in USVs are generally implemented at the software level within the main control system, which may become ineffective when the main system fails due to loss of communication, power instability, or unexpected errors [16], [17]. Furthermore, safety standards for autonomous vessels emphasize the importance of incorporating independent and reliable fail-safe mechanisms to ensure operational safety [18], [19].

Although autonomous USV technology is advancing rapidly, ensuring operational safety during abnormal conditions remains a significant challenge. Most existing safety systems are implemented directly within the main controller or autopilot system. Consequently, when the main controller experiences a malfunction, communication failure, or software instability, the safety mechanisms may also become unavailable [16], [17]. Furthermore, previous research has generally focused only on battery monitoring or communication recovery separately without integrating an independent safety architecture capable of autonomous decision making [9], [12].

These limitations reduce the reliability and resilience of USV operations, particularly in long-term missions and maritime environments with limited communication [13], [19]. Unlike conventional fail-safe implementations that only monitor predefined voltage thresholds, the

Setyawan Ajie Sukarno. Department of Automation Engineering, Politeknik Manufaktur Bandung, Bandung, 40135, Indonesia. E-mail: ajie@ae.polman-bandung.ac.id
Hisyam Nuruliman. Department of Automation Engineering, Politeknik Manufaktur Bandung, Bandung, 40135, Indonesia. E-mail: hisyamnurul216@gmail.com
Ridwan. Department of Automation Engineering, Politeknik Manufaktur Bandung, Bandung, 40135, Indonesia. E-mail: ridwan@ae.polman-bandung.ac.id

proposed system combines independent hardware-based monitoring, MAVLink heartbeat supervision, and mission-progress-based energy feasibility estimation within a unified autonomous safety framework. This approach enables proactive fail-safe decision making rather than conventional reactive threshold-based protection, thereby improving operational reliability during abnormal conditions.

The novelty of this research lies in the implementation of an ESP32-based fail-safe architecture that operates independently from the onboard main controller. The proposed system integrates progress-based energy estimation, MAVLink heartbeat-based communication monitoring, and real-time battery monitoring into a unified fail-safe decision-making framework. The proposed design enables autonomous safety monitoring and fail-safe execution even when onboard communication or processing becomes unreliable, unlike traditional methods that rely solely on the main controller [16], [17]. This strategy aligns with the concept of fault-tolerant system design, which emphasizes independent monitoring and reliable operation under abnormal conditions [13], [14], [15].

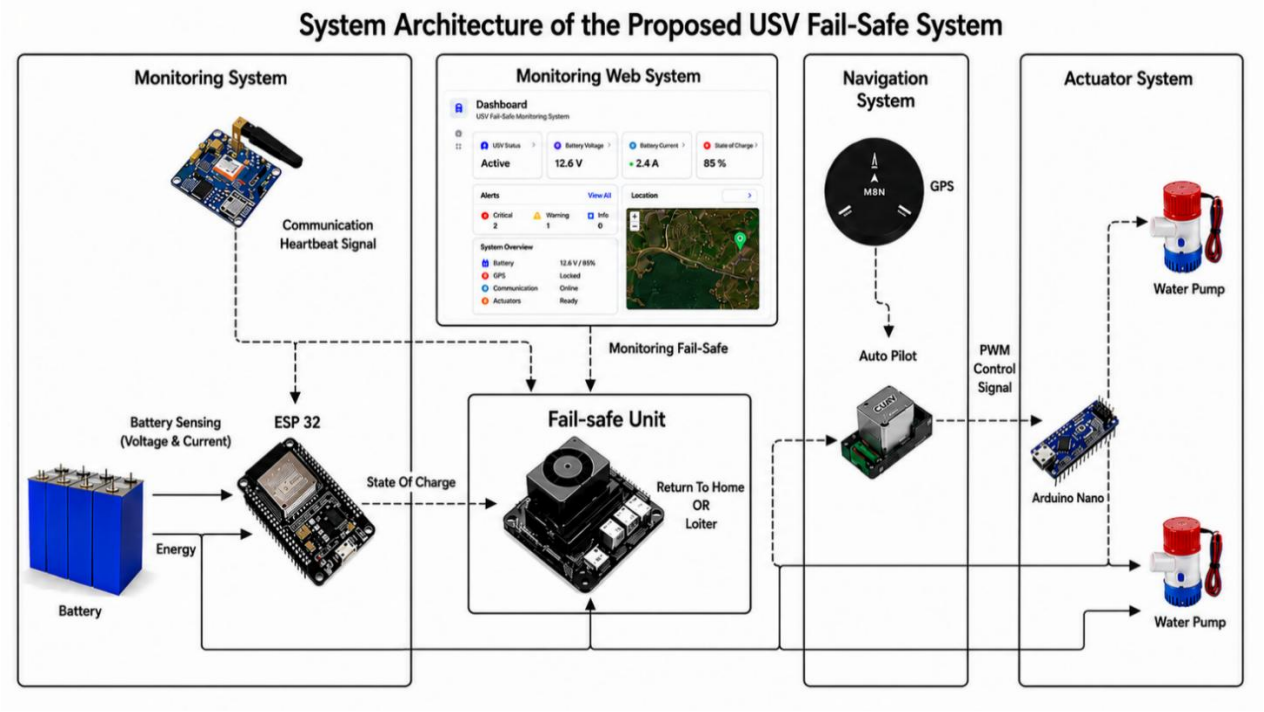

Figure 1. System Architecture of the Proposed USV Fail-Safe System

Therefore, this study proposes the design and implementation of an independent battery and lost-link fail-safe module to improve the operational safety and reliability of Unmanned Surface Vehicles (USVs). The proposed system continuously monitors battery conditions and communication status while autonomously executing fail-safe actions, including Return-to-Home (RTH) and Loiter modes, under abnormal operating conditions. Unlike conventional approaches that rely on the primary onboard controller, the proposed architecture separates the monitoring and decision-making subsystem from the main control system, thereby improving fault tolerance, system robustness, and operational safety in autonomous maritime applications [13], [18], [19].

The remainder of this paper is organized as follows. Section II presents the proposed system architecture and methodology. Section III discusses the experimental results and system evaluation. Finally, Section IV concludes the paper and outlines future research directions.

II. METHOD

A. System Architecture

The proposed Unmanned Surface Vehicle (USV) system consists of three main layers: (1) the autopilot layer, (2) the high-level computing layer, and (3) the independent fail-safe monitoring layer, as illustrated in Fig. 1. This layered architecture is designed to enhance system reliability by separating critical monitoring functions from the main control system [12], [13], [18].

The autopilot layer, implemented using the CUAV autopilot, is responsible for handling low-level control tasks, including waypoint navigation, heading stabilization, and actuator signal generation. Such low-level control is essential in autonomous marine systems to ensure stable navigation and motion control [1], [12].

The high-level computing layer is implemented using the Jetson Orin Nano, which handles telemetry processing, mission management, data communication, and high-level decision-making support. This layer receives navigation and system data from the autopilot while exchanging monitoring information with the autonomous safety module.

The independent monitoring layer is implemented using an ESP32 microcontroller due to its low power

consumption, integrated wireless communication capabilities, and sufficient computational resources for real-time monitoring applications. The ESP32 continuously collects battery voltage data and monitors communication status via MQTT heartbeat signals. This layer operates independently of the main computing unit, ensuring that critical system parameters can still be monitored even in the event of main system failure, which is a key principle in fault-tolerant system design [13], [14].

The overall system operates through continuous data exchange between layers. The ESP32 transmits battery status and trigger signals, while the Jetson processes telemetry data received from the autopilot. Based on this information, the system evaluates operational conditions and automatically determines whether fail-safe actions such as Return-to-Home (RTH) or Loiter mode activation are required.

B. Hardware Design

The hardware design of the proposed USV focuses on the implementation of sensing and actuation components that support reliable monitoring and control during operation. The main hardware components include an ESP32 microcontroller, a battery voltage and current sensing circuit, and actuator driver modules.

The battery voltage is measured using a voltage divider circuit connected to the analog-to-digital converter (ADC) of the ESP32. This circuit scales down the battery voltage to a measurable range suitable for the microcontroller. The output voltage of the divider is expressed as:

$$V_{out} = V_{in} \times \frac{R_2}{R_1+R_2} \quad (1)$$

Where Vin represents the actual battery voltage, while Vout is the scaled voltage read by the ADC. A calibration factor is applied in software to improve measurement accuracy [16].

Current measurement is performed using a Hall-effect current sensor (ACS712-30A), which provides an analog voltage proportional to the measured current. The current value is calculated using:

$$I = \frac{V_{out}-V_{offset}}{Sensitivity} \quad (2)$$

Where Vout is the measured sensor voltage, 2.5 V is the offset voltage, and 0.066 V/A is the sensitivity of the ACS712-30A sensor [17].

The battery monitoring hardware is designed to acquire real-time voltage and current data for energy estimation and fail-safe decision making. Voltage measurement is implemented using a voltage divider circuit combined with the ADS1115 analog-to-digital converter, while current measurement utilizes the ACS712 Hall-effect current sensor. The ADS1115 communicates with the ESP32 through the I2C interface, enabling reliable multi-channel data acquisition with improved measurement resolution and stability. These sensing components are integrated with the ESP32 microcontroller for data processing and monitoring, as illustrated in Figure 2.

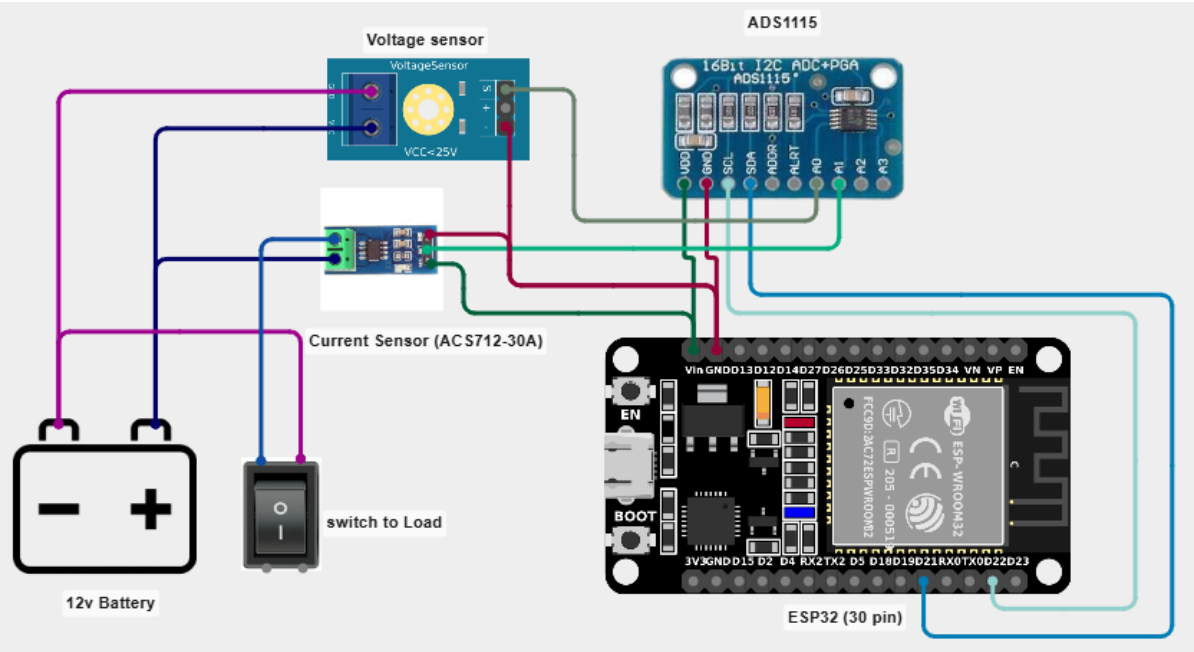

Figure 2. Hardware Design of the Battery Monitoring System

The actuator system consists of driver circuits controlled by PWM signals generated by the autopilot. These drivers regulate the operation of water thrusters, converting control signals into mechanical motion. Overall, the integration of ADS1115 enhances measurement precision and system reliability, making it suitable for real-time monitoring in autonomous marine applications [10], [11].

C. Software Design

The software design is implemented as a continuous loop consisting of data acquisition, processing,

communication, and system monitoring. The ESP32 initializes the ADS1115 via the I2C interface and establishes communication with the high-level computing unit through an MQTT-based messaging system [20].

Sensor data, including voltage and current measurements, are periodically acquired and processed before being published to the MQTT broker. The Jetson-based high-level computing unit subscribes to these data streams and processes them alongside telemetry data obtained from the autopilot via MAVLink communication [21], [22].

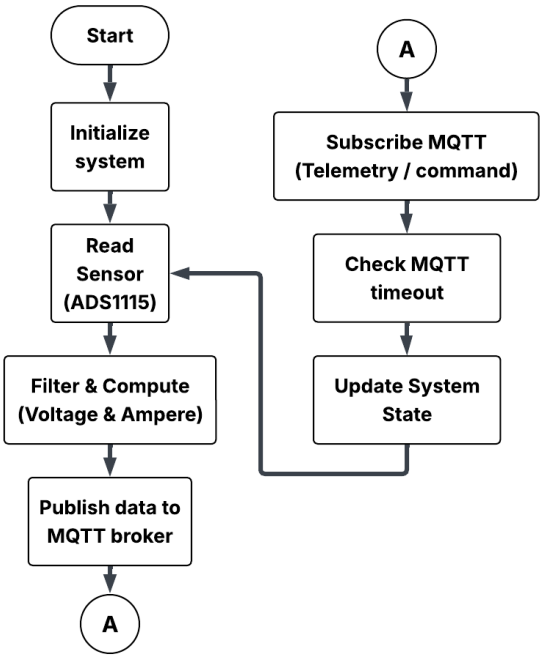

Figure 3. Software Operation Flow

In addition to publishing sensor data, the ESP32 also subscribes to MQTT topics to receive system status or telemetry information from the Jetson. Communication monitoring is performed by evaluating the reception of MQTT messages within a predefined timeout interval. If no messages are received within this interval, the system interprets this condition as a communication failure.

This bidirectional MQTT communication enables decoupled data exchange between system layers while maintaining real-time monitoring of communication integrity, which is a common approach in IoT-based monitoring systems [20], [23].

D. Fail-Safe Mechanism

The proposed fail-safe mechanism is designed to ensure safe operation of the USV by continuously monitoring system conditions and executing appropriate safety actions when abnormal situations are detected [26], [27]. The system integrates battery monitoring and communication reliability into a unified decision-making framework.

As illustrated in Fig. 4, the system operates in a continuous monitoring loop. Initially, the system performs initialization of the Battery Management System (BMS), autopilot, and telemetry communication. During operation, system data are continuously acquired from the BMS and autopilot, including battery status and communication signals.

The monitoring process consists of two parallel evaluations: energy monitoring and communication monitoring. The energy monitoring subsystem evaluates the battery condition, while the communication monitoring subsystem checks the availability of MAVLink heartbeat signals from the autopilot.

Communication status is determined based on the time interval between consecutive heartbeat signals. Let Δt denote the elapsed time since the last received heartbeat:

$$\Delta_t = t_{current} - t_{last} \quad (3)$$

where Δt is the elapsed time since the last heartbeat and Tth is the timeout threshold.

$$Status_{comm} = \begin{cases} Normal, & \Delta_t \le T_{th} \\ Lost\ Link, & \Delta_t > T_{th} \end{cases} \quad (4)$$

where Tth is the predefined timeout threshold, set to 15 seconds in this study. This value is selected considering the typical MAVLink heartbeat frequency of approximately 1 Hz, allowing the system to tolerate multiple missed messages while ensuring timely detection of link failure [20].

The battery voltage Vbat is measured using an ADC-based sensing circuit and serves as the primary input for estimating the battery condition [28], [29]. The system uses a $LiFePO_4$ battery, which exhibits a relatively flat discharge curve and high thermal stability [19]. Therefore, the State of Charge (SOC) is estimated from the measured voltage using a piecewise linear approximation [21].

$$SOC(V) = \begin{cases} 100, & V \ge 13.4 \\ 80 + \frac{V-12.8}{13.4-12.8} \times 20, & 12.8 \le V < 13.4 \\ 60 + \frac{V-12.4}{12.8-12.4} \times 20, & 12.4 \le V < 12.8 \\ 40 + \frac{V-12.2}{12.4-12.2} \times 20, & 12.2 \le V < 12.4 \\ 20 + \frac{V-12.0}{12.2-12.0} \times 20, & 12.0 \le V < 12.2 \\ \frac{V-11.4}{12.0-11.4} \times 20, & 11.4 \le V < 12.0 \\ 0, & V < 11.4 \end{cases} \quad (5)$$

The battery condition is evaluated based on mission feasibility using a progress-based energy estimation. The system estimates the energy consumption rate from the ratio between consumed energy and mission progress, and predicts the required energy to complete the remaining mission. A safety factor is incorporated to account for uncertainties such as environmental disturbances and sensor noise. The battery is considered sufficient when the remaining energy exceeds the estimated required energy;

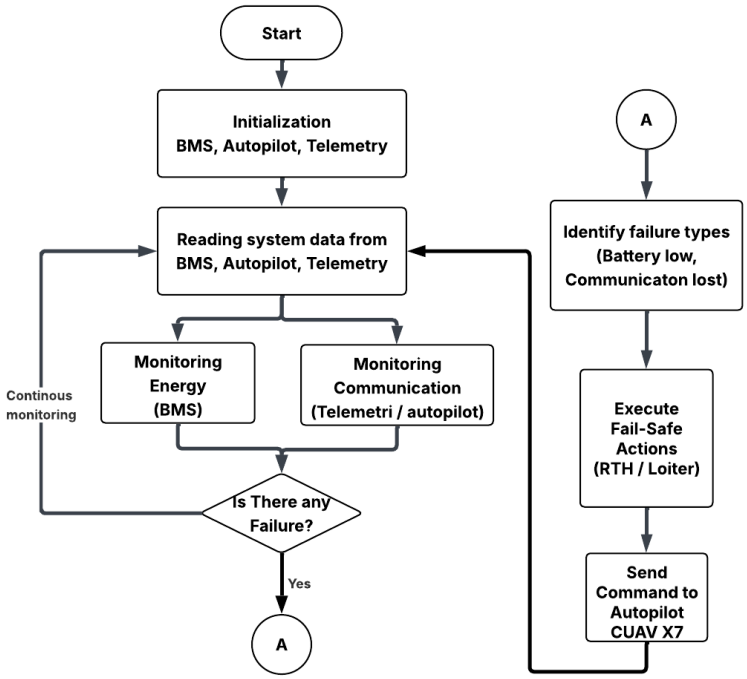

Figure 4. Fail-Safe Mechanism Flow

$$E_{rate} = \frac{E_{used}}{P} \quad (6)$$

$$E_{req} = (100 - P) \times E_{rate} \times \gamma \quad (7)$$

$$E_{rem} = E_{Total} - E_{Used} \quad (8)$$

Where Eused is the consumed energy (Wh), P is the mission progress (%), Erate is the energy consumption rate, Ereq is the required remaining energy, γ is the safety factor. A safety factor of γ =1.2 is applied to account for uncertainties. The selected safety factor provides additional energy reserve to compensate for environmental disturbances, sensor uncertainty, and dynamic operating conditions commonly encountered in maritime environments.

The proposed estimation assumes approximately linear energy consumption with respect to mission progress under relatively stable operating conditions and constant propulsion characteristics. The battery status is determined as:

$$Battery\ Status = \begin{cases} sufficient, & E_{rem} \geq E_{req} \\ insufficient, & E_{rem} < E_{req} \end{cases} \quad (9)$$

To avoid instability at the initial stage (P→0), the estimation is activated after a minimum progress threshold. The model assumes a linear relationship between energy consumption and mission progress. When the battery is classified as insufficient, a fail-safe response such as mission abort or return-to-home is triggered. This mechanism enables a hierarchical fail-safe strategy that combines real-time monitoring, condition-based evaluation, and autonomous response, thereby improving system robustness and operational safety.

E.Experimental Testing

The experiments were conducted in open waters to evaluate the system's performance under actual operating conditions. The system utilizes voltage and current sensors to estimate energy consumption in real time, combined with a progress-based method to predict the required energy for mission completion.

Three experimental scenarios were designed as summarized in Table 1. Each scenario was repeated multiple times to evaluate consistency and reliability of the fail-safe responses under different operational conditions.

TABLE 1.
EXPERIMENTAL SCENARIOS FOR FAIL-SAFE VALIDATION

Scenarios	Initial Condition	Disturbance	Objective	Expected Response
Normal Mission	Soc > 80%	None	Validate Nominal Operation	No Fail-Safe Triggered
Insufficient Battery	Soc < 40%	High Energy Demand	Detect Infeasible Mission	Trigger Return To Home
Communication Lost	Stable Operation	Telemetry Disconnected	Validate Communication Fail-Safe	Trigger Loiter & Return To Home

The system performance was evaluated based on estimation accuracy and decision reliability. The estimated energy consumption and remaining energy were compared with actual measurements to assess prediction accuracy. Additionally, the correctness of fail-safe decisions was analyzed by comparing system outputs with actual mission outcomes. A web-based monitoring interface is used during the experiment to visualize real-time system parameters, including battery status, and fail-safe conditions, as shown in Figure 5.

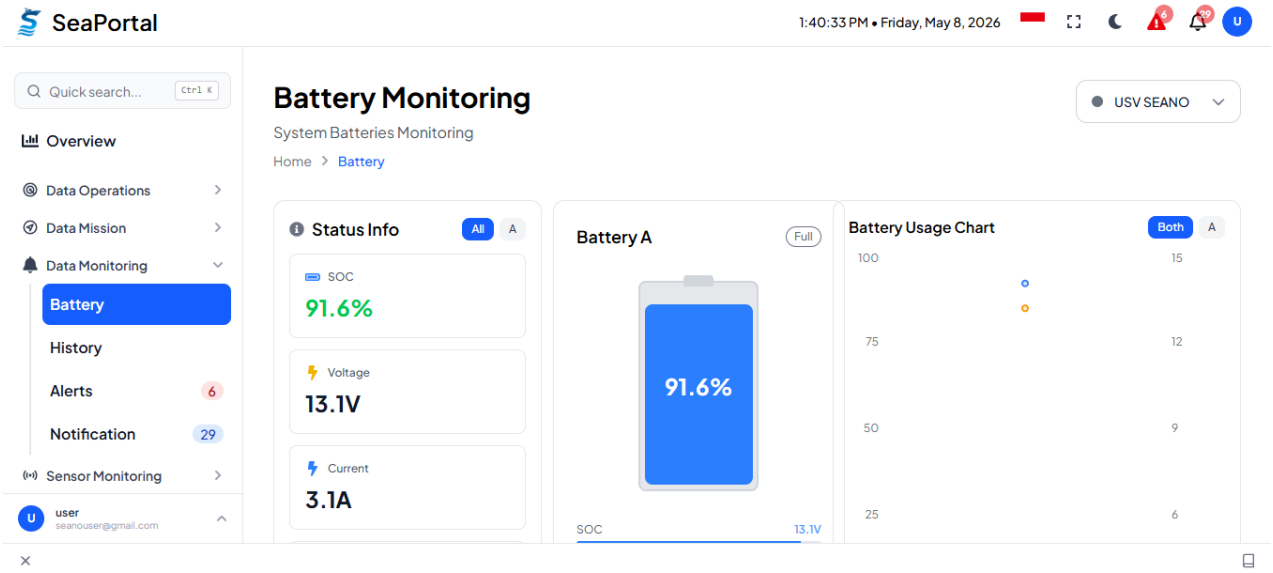

Figure 5. Web-Based Monitoring Interface for Battery and Fail-Safe System.

III. Results and Discussion

The results are organized into four main aspects, including battery monitoring performance, communication performance, fail-safe scenario validation, and system monitoring visualization. The experiments were carried out at Lake Lembah Dewata, Lembang, representing a real-world open-water environments that introduces practical challenges such as signal attenuation, environmental disturbances, and varying communication ranges, thereby enabling comprehensive evaluation of the system performance.

Figure 6. Experimental Testing of the Proposed USV Prototype

A. Battery Monitoring Performance

The voltage measurement results are presented in Table 2. The measurements obtained from the voltage divider and ADS1115 are compared with a reference voltmeter to evaluate accuracy. The results show that the proposed sensing circuit provides stable and consistent readings across different measurement instances.

The average voltage deviation is approximately 0.02 V, with a mean absolute percentage error (MAPE) of 0.13%. The overall measurement accuracy reaches

99.87%, indicating that the system is capable of providing reliable voltage data for battery monitoring.

The high measurement accuracy demonstrates that the proposed sensor architecture is sufficiently reliable for real-time maritime safety applications. Compared to conventional low-cost ADC implementations integrated directly into microcontrollers, the ADS1115-based measurement system improves voltage stability and supports more reliable fail-safe decision-making.

Although small deviations are observed in some measurements, with a maximum error of 0.23%, these variations are still within an acceptable range for real-time monitoring applications. The results confirm that the integration of a voltage divider with the ADS1115 ADC offers sufficient precision for use in the proposed fail-safe system. These results indicate that the proposed monitoring system is capable of maintaining stable measurement performance under practical operational conditions, which is essential for ensuring reliable energy estimates during autonomous USV missions.

B. Communication Performance

The communication system is evaluated based on latency, packet loss, and timeout-based detection to assess its reliability and robustness. In addition, the system response under communication failure is analyzed through the implemented fail-safe mechanism. The experimental results are presented in Table 3.

TABLE 2.
VOLTAGE MEASUREMENT

NO	TIME	VOLTAGE DIVIDER (V)	VOLTMETER (V)	DIFFERENCE (V)	ERROR (%)	ACCURACY (%)
1	21:50	13.23	13.2	0.03	0.23%	99.77%
2	21:51	13.23	13.2	0.03	0.23%	99.77%
3	21:52	13.22	13.2	0.02	0.15%	99.85%
4	21:53	13.22	13.2	0.02	0.15%	99.85%
5	21:54	13.21	13.2	0.01	0.08%	99.92%
6	10:12	13.16	13.15	0.01	0.08%	99.92%
7	10:13	13.16	13.15	0.01	0.08%	99.92%
8	10:14	13.15	13.14	0.01	0.08%	99.92%
9	10:15	13.15	13.14	0.01	0.08%	99.92%
10	10:16	13.14	13.13	0.01	0.08%	99.92%
11	10.45	13.13	13.12	0.01	0.08%	99.92%
12	10.46	13.13	13.12	0.01	0.08%	99.92%
13	10.47	13.13	13.12	0.01	0.08%	99.92%
14	10.48	13.12	13.10	0.02	0.15%	99.85%
15	10.49	13.12	13.10	0.02	0.15%	99.85%
16	11.35	13.03	13.00	0.03	0.23%	99.77%
17	11.36	13.03	13.00	0.03	0.23%	99.77%
18	11.37	13.02	13.00	0.02	0.15%	99.85%
19	11.38	13.02	13.00	0.02	0.15%	99.85%
20	11.39	13.02	13.00	0.02	0.15%	99.85%
		Mean		0.02	0.13%	99.87%
		Mean Absolute Percentage Error (MAPE)				0.13%

When the communication link is completely lost, latency cannot be measured due to the absence of incoming data packets, thus it is represented as N/A. However, the system continues to monitor the elapsed time since the last successful communication (Δt). If this duration exceeds a predefined threshold, the system classifies the condition as lost link and activates the fail-safe mechanism.

The communication evaluation shows that the proposed heartbeat-based supervision mechanism is capable of distinguishing between communication disruptions and total connection failures. This capability is particularly important in maritime environments, where sporadic packet loss and unstable telemetry are common due to environmental interference and long communication distances.

The timeout-based detection strategy also enhances system resilience by preventing premature fail-safe activation during temporary communication disruptions, thereby reducing the possibility of unnecessary mission interruption.

C. Fail-Safe Scenario Validation

The fail-safe scenario validation was conducted to evaluate the system's ability to detect abnormal conditions and execute appropriate safety actions. The tested scenarios include normal operation, low battery conditions, and communication loss (lost link). The detailed results of the fail-safe scenario validation are summarized in Table 4.

Under normal conditions, the system maintained a stable connection with low communication delay (Δt < 1

s), and no fail-safe mechanism was triggered, indicating proper system operation.

In low battery scenarios, the system successfully detected the energy threshold violation within 2.5–3.0 seconds and activated the fail-safe mechanism by initiating a Return-to-Home (RTH) action. The response demonstrates that the energy-based monitoring system can effectively prevent mission continuation under unsafe battery conditions.

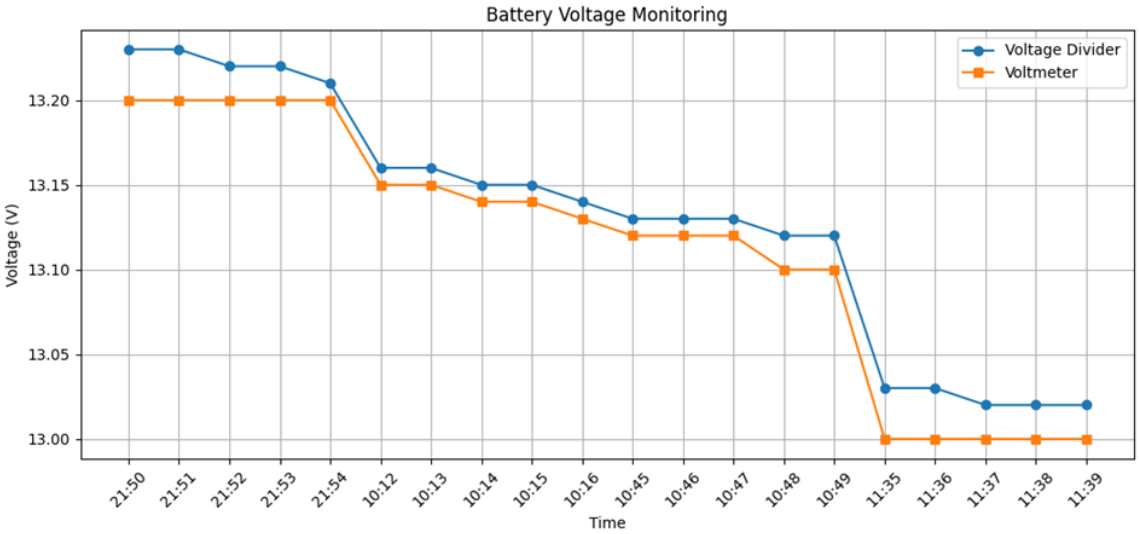

Figure 7. Comparison of Measured Voltage Between Proposed Sensor and Reference Voltmeter

TABLE 4.
FAIL-SAFE SCENARIO VALIDATION

TRIAL	Δ_t (s)	DETECTION TIME (s)	SOC (%)	STATUS	FAIL-SAFE	ACTION	EXPECTED ACTION	RESULT
1	1.7	-	86.1	CONNECTED	FALSE	NONE	NONE	✔
2	1.4	-	85.9	CONNECTED	FALSE	NONE	NONE	✔
3	1.3	-	83.6	CONNECTED	FALSE	NONE	NONE	✔
1	1.2	2.6	50%	CONNECTED	TRUE	RTH	RTH	✔
2	1.5	2.6	45%	CONNECTED	TRUE	RTH	RTH	✔
3	1.5	2.8	40%	CONNECTED	TRUE	RTH	RTH	✔
1	6.2	5.0	88%	DISCONNECTED	TRUE	LOITER	LOITER	✔
2	13.4	5.0	86%	DISCONNECTED	TRUE	LOITER	LOITER	✔
3	16.5	15.0	80%	DISCONNECTED	TRUE	RTH	RTH	✔

For communication loss scenarios, the system experienced disconnection with Δt exceeding 6 seconds or becoming unavailable. The fail-safe mechanism was consistently triggered, and the system executed a loiter action as expected. The detection time ranged from 6.2 to 15.0 seconds, depending on communication delay conditions.

Overall, the system demonstrated reliable performance in all tested scenarios, with all fail-safe actions matching the expected responses, confirming the effectiveness of the proposed safety mechanism.

The experimental results confirm that the proposed independent fail-safe architecture improves operational resilience compared with conventional controller-dependent safety systems. Since the ESP32 monitoring subsystem operates independently from the main onboard computer, the fail-safe function remains active even when the main telemetry or the processing system becomes unstable.

Furthermore, the integration of mission-progress-based energy estimation enables proactive fail-safe decision making rather than simple threshold-based protection. Instead of reacting only to low voltage conditions, the system evaluates whether the remaining energy is sufficient to complete the mission safely. This approach improves operational safety by preventing mission continuation under infeasible energy conditions before critical battery depletion occurs.

D. System Monitoring Via Web Interface

The web-based monitoring interface was successfully developed to provide real-time visualization of system

parameters and operational status. As shown in Fig. 8, the interface presents essential battery information, including state of charge (SOC), voltage, current, and capacity, accompanied by a graphical representation of battery usage over time. This visualization enables continuous observation of the system's energy condition during mission execution.

In addition to parameter visualization, the system incorporates an alert mechanism to indicate critical operational conditions. When a fail-safe event is triggered due to communication loss, the monitoring interface generates a critical alert notification. As illustrated in Fig. 9, fail-safe events such as COMM_LOST_RTL and COMM_LOST_LOITER are clearly displayed on the dashboard, allowing operators to promptly identify the type of failure and respond accordingly.

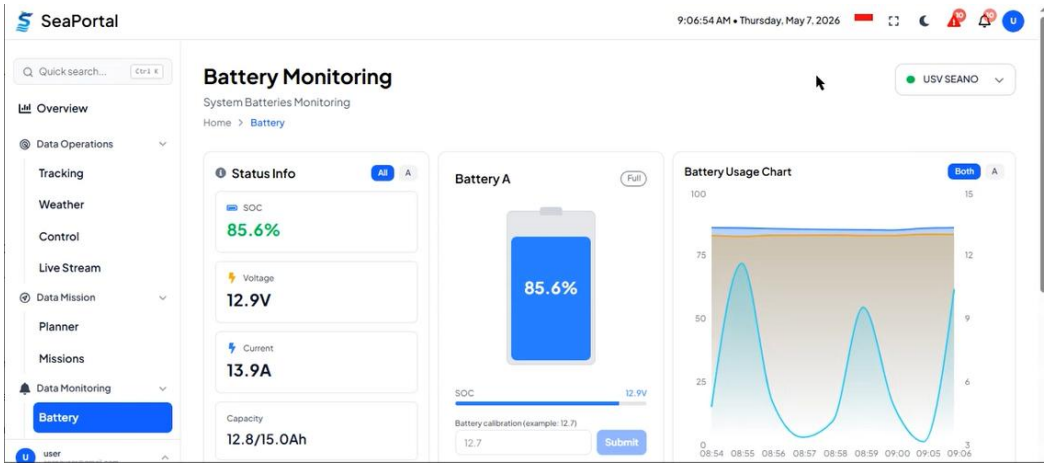

Figure 8. Battery Monitoring Dashboard

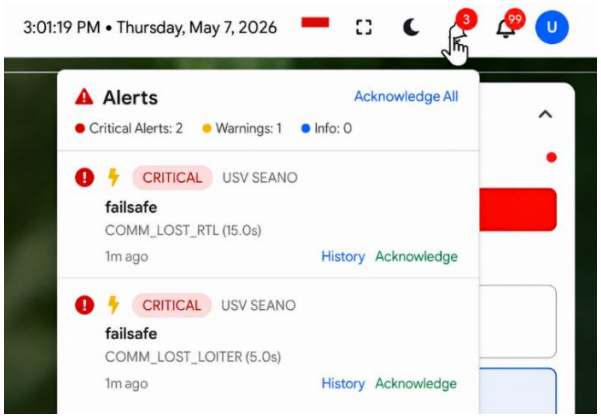

Figure 9. Fail-Safe Communication Loss Alert on Monitoring Dashboard

Furthermore, the system is capable of detecting energy-related fail-safe conditions. When the available battery energy is predicted to be insufficient to complete the mission, a critical alert labeled ENERGY_NOT_ENOUGH is generated and displayed in real time. This condition is visualized in Fig. 10, where the alert notification indicates a critical energy limitation during operation.

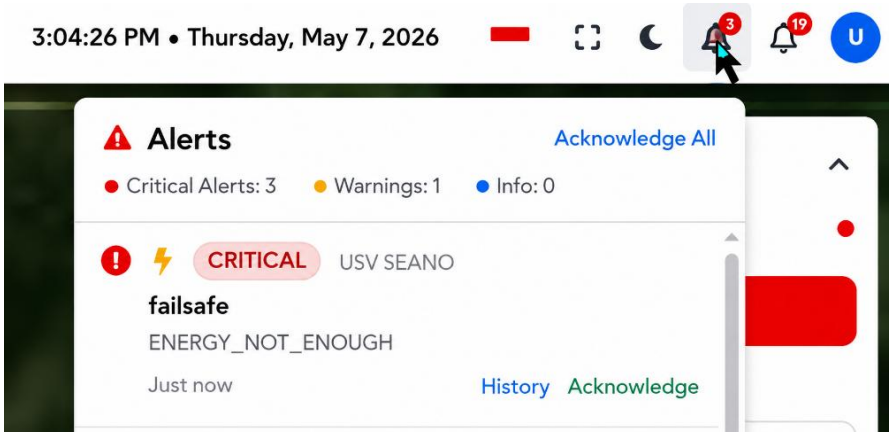

Figure 10. Fail-Safe Energy Not Enough Alert on Monitoring Dashboard

Overall, the proposed web-based monitoring interface effectively integrates real-time data visualization and fail-safe alert notifications, thereby supporting timely decision-making and improving system reliability during operation. The integration of real-time monitoring and fail-safe alert visualization also improves operator situational awareness during autonomous operation. This capability is particularly important in remote maritime missions where rapid identification of abnormal conditions is required to reduce operational risk. In addition to providing visualization, the effectiveness of the proposed system is further validated through scenario-based testing results.

The results demonstrate that the proposed method is capable of predicting mission feasibility with acceptable accuracy. In the insufficient battery scenario, the system successfully triggered the fail-safe mechanism before the battery reached a critical level, thereby preventing potential mission failure. Furthermore, in the communication loss scenario, the system demonstrated the ability to autonomously respond to connection failures, ensuring safe and stable operation.

These results confirm that the integration of real-time monitoring, energy estimation, and condition-based decision-making significantly enhances system reliability and operational safety. Compared with conventional monitoring approaches that only provide passive parameter visualization, the proposed system integrates autonomous condition evaluation and fail-safe response into a unified monitoring framework. This integration enhances autonomous maritime operational resilience.

IV. Conclusion

This paper presents the design and implementation of an independent battery and lost-link fail-safe module for improving the operational safety of Unmanned Surface Vehicles (USVs). The proposed system utilizes a multi-layer architecture that separates monitoring, control, and decision-making functions to improve system reliability and fault tolerance. Unlike conventional fail-safe systems that depend on the main onboard controller, the proposed ESP32-based architecture enables continuous fail-safe operation even when the main communication or processing system becomes unstable.

In addition, the integration of mission-progress-based energy estimation enables proactive safety evaluation beyond conventional threshold-based approaches. Experimental results demonstrate that the proposed system achieved 99.87% battery monitoring accuracy and successfully detected low battery and communication loss conditions within acceptable response times. The fail-safe mechanism was able to execute appropriate actions, including Return-to-Home (RTH) and Loiter modes, while the web-based monitoring interface improved situational awareness through real-time visualization and alert notifications.

Overall, the proposed system enhances the operational resilience and safety of USVs operating in remote and communication-limited open-water environments. Future work may focus on improving prediction accuracy using advanced machine learning methods and extending the system to multi-vehicle coordination scenarios.

Acknowledgements

The authors would like to express their sincere gratitude to the Ministry of Higher Education, Science, and Technology of the Republic of Indonesia (Kemdiktisaintek) for the financial support provided for this research. The authors also appreciate all parties who contributed to the completion of this study.

References

[1] X. Wang, Y. Ouyang, X. Wang, and Q. Wang, “A Novel, Finite-Time, Active Fault-Tolerant Control Framework for Autonomous Surface Vehicle with Guaranteed Performance,” Journal of Marine Science and Engineering, vol. 12, no. 2, Art. no. 347, Feb. 2024, doi: 10.3390/jmse12020347.

[2] C. Barrera, I. Padron, F. S. Luis, O. Llinas, and G. N. Marichal, “Trends and challenges in unmanned surface vehicles (USV): From survey to shipping,” TransNav: The International Journal on Marine Navigation and Safety of Sea Transportation, vol. 15, no. 1, pp. 135–142, Mar. 2021, doi: 10.12716/1001.15.01.13.

[3] F. Sotelo-Torres, L. V. Alvarez, and R. C. Roberts, “An Unmanned Surface Vehicle (USV): Development of an Autonomous Boat with a Sensor Integration System for Bathymetric Surveys,” Sensors, vol. 23, no. 9, Art. no. 4420, Apr. 2023, doi: 10.3390/s23094420.

[4] S. D. Kristensen, A. Dallolio, and I. B. Utne, “A Systems Approach to Hazard Identification for Solar-Powered and Wave-Propelled Unmanned Surface Vehicle,” Journal of Marine Engineering and Technology, vol. 23, no. 2, pp. 122–134, 2024, doi: 10.1080/20464177.2024.2315646.

[5] C. Kooij, A. A. Kana, and R. G. Hekkenberg, “A task-based analysis of the economic viability of low-manned and unmanned cargo ship concepts,” Ocean Engineering, vol. 242, Art. no. 110111, Dec. 2021, doi: 10.1016/j.oceaneng.2021.110111.

[6] V. Bolbot, A. Sandru, T. Saarniniemi, O. Puolakka, P. Kujala, and O. A. Valdez Banda, “Small Unmanned Surface Vessels—A Review and Critical Analysis of Relations to Safety and Safety Assurance of Larger Autonomous Ships,” Journal of Marine Science and Engineering, vol. 11, no. 12, Art. no. 2387, Dec. 2023, doi: 10.3390/jmse11122387.

[7] Z. Lv, X. Wang, G. Wang, X. Xing, C. Lv, and F. Yu, “Unmanned Surface Vessels in Marine Surveillance and Management: Advances in Communication, Navigation, Control, and Data-Driven Research,” Journal of Marine Science and Engineering, vol. 13, no. 5, Art. no. 969, May 2025, doi: 10.3390/jmse13050969.

[8] J. D. Setiawan, M. A. Septiawan, M. Ariyanto, W. Caesarendra, M. Munadi, S. Alimi, and M. Sulowicz, “Development and Performance Measurement of an Affordable Unmanned Surface Vehicle (USV),” Automation, vol. 3, no. 1, pp. 27–46, Jan. 2022, doi: 10.3390/automation3010002.

[9] S. H. Kim, J. W. Jung, M. Y. Jang, and S. J. Kim, “Extended Probabilistic Risk Assessment of Autonomous Underwater Vehicle Docking Scenarios Considering Battery Consumption,” Journal of Marine Science and Engineering, vol. 13, no. 9, Art. no. 1714, Sep. 2025, doi: 10.3390/jmse13091714.

[10] Y. V. Korotaev, A. V. Leonov, and A. A. Kapustin, “Development of a High-Reliability Hybrid Data Transmission System for Unmanned Surface Vehicles Under Interference Conditions,” Drones, vol. 9, no. 3, Art. no. 174, 2025, doi: 10.3390/drones9030174.

[11] A. A. Priadi, T. Cahyadi, L. Barasa, S. A. Sukarno, N. Suranta, and M. Yando, “Development of IoT-Based Monitoring for Unmanned Surface Vessels (USV),” Journal of Engineering Science and Technology, Special Issue on STIPCON2024, vol. 20, no. 5, pp. 1–10, 2025. [Online]. Available: https://jestec.taylors.edu.my/Special%20Issue%20STIPCON2024/STIPCON%202024_1.pdf

[12] A. Avizienis, J.-C. Laprie, B. Randell, and C. Landwehr, “Basic Concepts and Taxonomy of Dependable and Secure Computing,” IEEE Transactions on Dependable and Secure Computing, vol. 1, no. 1, pp. 11–33, Jan.–Mar. 2004, doi:

10.1109/TDSC.2004.2.

[13] I. Koren and C. M. Krishna, Fault-Tolerant Systems, 1st ed. San Francisco, CA, USA: Morgan Kaufmann, 2007, ISBN: 9780120885251.

[14] J.-C. Laprie, Ed., Dependability: Basic Concepts and Terminology, Dependable Computing and Fault-Tolerant Systems, vol. 5. Vienna, Austria: Springer Vienna, 1992, doi: 10.1007/978-3-7091-9170-5.

[15] H. Park, J. Kim, M. Jung, S.-Y. Kang, D. Kim, C. Kim, and U. Jang, "Risk Management Challenges in Maritime Autonomous Surface Ships (MASSs): Training and Regulatory Readiness," Applied Sciences, vol. 15, no. 20, Art. no. 10993, Oct. 2025, doi: 10.3390/app152010993.

[16] T.-E. Kim, L. P. Perera, M.-P. Sollid, B.-M. Batalden, and A. K. Sydnes, "Safety challenges related to autonomous ships in mixed navigational environments," WMU Journal of Maritime Affairs, vol. 21, no. 2, pp. 141–159, 2022, doi: 10.1007/s13437-022-00277-z.

[17] Indian Register of Shipping, Guidelines on Remotely Operated Vessels and Autonomous Surface Vessels, IRS-G-DES-13, Dec. 2021. [Online]. Available: https://www.irclass.org/media/6394/gl_remotely-operated-vessels-autonomous-surface-vessels_irs-g-des-13_rev01_dec-2022.pdf

[18] N. G. Leveson, Engineering a Safer World: Systems Thinking Applied to Safety. Cambridge, MA, USA: MIT Press, 2011, ISBN: 9780262016629.

[19] A. Banks and R. Gupta, Eds., MQTT Version 3.1.1, OASIS Standard. OASIS, Oct. 2014. [Online]. Available: https://www.oasis-open.org/standard/mqttv3-1-1/

[20] G. L. Plett, Battery Management Systems, Volume I: Battery Modeling, 1st ed. Norwood, MA, USA: Artech House, 2015, ISBN: 9781630810238.

[21] M. Chen and G. A. Rincon-Mora, "Accurate Electrical Battery Model Capable of Predicting Runtime and I–V Performance," IEEE Transactions on Energy Conversion, vol. 21, no. 2, pp. 504–511, Jun. 2006, doi: 10.1109/TEC.2006.874229.

[22] U. Hunkeler, H. L. Truong, and A. Stanford-Clark, "MQTT-S—A Publish/Subscribe Protocol for Wireless Sensor Networks," in Proceedings of the 3rd International Conference on Communication Systems Software and Middleware and Workshops (COMSWARE), Bangalore, India, Jan. 2008, pp. 791–798, doi: 10.1109/COMSWA.2008.4554519.

[23] L. D. Xu, W. He, and S. Li, "Internet of Things in Industries: A Survey," IEEE Transactions on Industrial Informatics, vol. 10, no. 4, pp. 2233–2243, Nov. 2014, doi: 10.1109/TII.2014.2300753.

[24] S. Madakam, R. Ramaswamy, and S. Tripathi, "Internet of Things (IoT): A Literature Review," Journal of Computer and Communications, vol. 3, no. 5, pp. 164–173, May 2015, doi: 10.4236/jcc.2015.35021.

[25] J. Rushby, "Critical System Properties: Survey and Taxonomy," Reliability Engineering & System Safety, vol. 43, no. 2, pp. 189–219, 1994, doi: 10.1016/0951-8320(94)90065-5.

[26] N. Storey, Safety-Critical Computer Systems. Harlow, U.K.: Addison-Wesley, 1996, ISBN: 9780201427875.

[27] R. R. Murphy, Introduction to AI Robotics. Cambridge, MA, USA: MIT Press, 2000, ISBN: 9780262133838.

[28] P. Horowitz and W. Hill, The Art of Electronics, 3rd ed. Cambridge, U.K.: Cambridge University Press, 2015, ISBN: 9780521809269.

[29] T. B. Reddy, Ed., Linden's Handbook of Batteries, 4th ed. New York, NY, USA: McGraw-Hill, 2011, ISBN: 9780071624213